Journal of Photochemistry and Photobiology A: Chemistry 219 (2011) 255–264

Contents lists available at ScienceDirect

Journal of Photochemistry and Photobiology A: Chemistry

journal homepage: www.elsevier.com/locate/jphotochem

The 2-benzoyl xanthone/triethylamine system as a type **II** photoinitiator: A laser flash photolysis and computational study [1]

Xenophon Asvos[a], Michael G. Siskos[a,*], Antonios K. Zarkadis[a], Ralf Hermann[b], Ortwin Brede[b]

[a] *Department of Chemistry, University of Ioannina, 45110 Ioannina, Greece*
[b] *Wilhelm-Ostwald-Institute for Physical and Theoretical Chemistry, Faculty of Chemistry and Mineralogy, University of Leipzig, Permoserstr. 15, 04318 Leipzig, Germany*

ARTICLE INFO

Article history:
Received 12 November 2010
Received in revised form 24 February 2011
Accepted 28 February 2011
Available online 8 March 2011

Keywords:
Photochemistry
Photopolymerization
Type II photoinitiator
Photoinitiator quenching
Electron transfer

ABSTRACT

2-Benzoylxanthone (**BzX**) was synthesized, characterized and used as type II photoinitiator (**PI**) in combination with triethylamine for the polymerization of methylmethacrylate (**MMA**). The photophysical/photochemical behaviour of the photoinitiator, the involved excited state and the reaction with the amine co-initiator was studied by means of absorption and nanosecond time-resolved absorption spectroscopy. Upon irradiation with 266 or 355 nm laser light, the triplet state ^{3}**BzX*** (λ_{max} = 355 nm and 530 nm) was generated as the only transient (lifetime of 22.7 μs) in nitrogen saturated MeCN solution. ^{3}**BzX*** was confirmed through quenching experiments with oxygen, 2-methylbutadiene, perylene and **MMA** and spectral similarity to benzophenone triplet (^{3}**BP***). The quantum yield of its formation (Φ_T = 0.8) and the molar absorption coefficient (ε = 7500 L mol^{-1} cm^{-1}) was measured in MeCN. The triplet was photoreduced by triethylamine (TEA) *via* photoinduced electron/proton transfer giving the corresponding ketyl and α-amino ethyl radical (•CHMe–NEt$_2$). From the reduction potential of **BzX** measured *via* cyclic voltametry (two cathodic peaks at −1.63 V and −1.91 V vs. Ag/AgCl), an exergonic electron transfer reaction results. The ketyl radical resembles the well-known benzophenone ketyl. In conclusion, the triplet ^{3}**BzX*** corresponds to an n → π* transition localized on the benzoyl substituent and resembles the benzophenone triplet ^{3}**BP*** but deviates from the triplet state of xanthone (^{3}**X***). This is supported through DFT/B3LYP calculations, *viz.*, (i) fully ground and triplet state geometry optimizations show that charge and spin densities are localized on the benzoyl group, and (ii) calculation of the electronic transitions *via* TD-DFT at B3LYP/631G+(d) and PB1BPE/631G+(d) levels of theory shows the local character. Agreement with experiment is better by applying the conductor like polarized continuum model (CPCM) to consider the solvent effect (MeCN).

The effectiveness of **BzX** as photoinitiator for the polymerization of **MMA** is found to be double that of the unsubstituted xanthone (**X**). The photopolymerization rates (R_p) were found to be 7.06 × 10^{-4} mol L^{-1} s^{-1} in the case of **BzX** and 3.04 × 10^{-4} mol L^{-1} s^{-1} in the case of **BX**. This is attributed to the fact that triplet ^{3}**BzX*** behaves like the benzophenone triplet ^{3}**BP*** and deviates from that of ^{3}**X***, i.e., it is the localization of the triplet excitation on the benzoyl subunit which renders **BzX** a good type-**II** photoinitiator.

1. Introduction

Photoinitiated polymerization is one of the most rapidly expanding processes because of its widespread applications in printing inks, adhesives, surface coating, microelectronics, printing plates, etc. [1–9]. A crucial component in all photopolymerization systems is the photoinitiator (**PI**) which absorbs light and generates the active radicals to initiate the polymerization. From the mechanistic point of view, there are two main categories of photoinitiators. Type **I** photoinitiators, which undergo direct photofragmentation upon absorption of light and afford radicals capable of inducing polymerization (e.g. benzoin ethers, acylphosphine oxides, hydroxyalkylphenyl ketones, dialkoxy acetophenones, alkyl amino ketones, sulfonyl ketones, silicon derivatives of ketones, etc.), and type **II** photoinitiating systems which are based on hydrogen transfer or electron transfer followed by proton transfer. The latter process takes place between the triplet excited state of the **PI** (usually an aromatic ketone, e.g., benzophenone and thioxanthone) and a coinitiator acting as hydrogen or electron/proton donor (e.g., a thiol or an amine), thereby producing the initiating radicals. Some of the properties needed to improve **PI** efficiency are high absorption coefficients, inefficient quenching of the relevant excited states by the monomer or oxygen and high quantum yields in producing the initiating radicals.

* Corresponding author. Tel.: +30 26510 08394; fax: +30 26510 08799.
E-mail address: msiskos@cc.uoi.gr (M.G. Siskos).

1010-6030/$ – see front matter © 2011 Elsevier B.V. All rights reserved.
doi:10.1016/j.jphotochem.2011.02.028

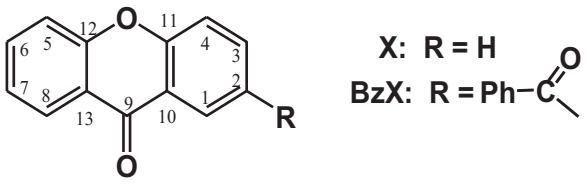

Scheme 1.

Consequently, the role of the photoinitiator efficiency is very crucial and therefore the search for novel compounds that can be used as photoinitiators has continuously received considerable attention in the last three decades. In order to improve the photoinitiator properties some aspects of these studies are focused in replacing the chromophore or in modifying the chromophore through the introduction of suitable substituents (donors or acceptors) on the same chromophore. A variety of substituted benzophenones or thioxanthones have been examined for this purpose and in some cases increased photoinitiation ability was found [10].

Although many substituents in aromatic ketones have been studied, nothing is known regarding the introduction of a second carbonyl group. Thus, in this work we intend to extend the chromophore of xanthone introducing a benzoyl group at the 2-position (**BzX**, Scheme 1), to look for its potential function as photoinitiator and to compare its activity against the unsubstituted xanthone. More precisely, in this work we perform a systematic study which focused: (i) to the photophysical and photochemical properties using steady state absorption/emission and laser flash photolysis techniques, (ii) to compare the photoinitiation activity of the substituted and unsubstituted xanthone (polymerization of **MMA** using **Et_3N** as co-initiator), (iii) to the quenching of the excited state of PIs by triethylamine and monomer (**MMA**), and (iv) to shed light to mechanistic questions related to the specific role played by each carbonyl group. We have also performed quantum mechanical calculations examining the geometry of the ground and triplet excited states, as well as, the relevant molecular orbitals and electronic transitions (PM3, AM1, Ab initio and DFT and TD-DFT) in order to support the interpretation of the obtained results.

The present results show that 2-benzoyl xanthone (**BzX**) functions as a type-**II** photoinitiator with an effectiveness twice as that of the unsubstituted xanthone (**X**) for the polymerization of **MMA**. As the spectral characteristics (photophysical, laser flash photolysis and computational results) indicate, this is attributed to the fact that triplet excitation of **BzX** is localized on the benzoyl subunit rather than on the xanthonyl part. Thus, the triplet ^{3}**BzX*** resembles the benzophenone triplet ^{3}**BP*** showing inefficient quenching by the monomer **MMA**, undergoing, however, a very competitive electron/proton transfer reaction with the co-initiator **Et_3N** which affords the desired initiating α-aminoethyl radical. In contrast, the quenching of xanthone triplet ^{3}**X*** by **MMA** is more competitive compared to the crucial electron transfer step, diminishing thus its polymerization ability.

2. Experimental

2.1. Materials

Acetonotrile, cyclohexane and MeOH (all spectroscopic grades) were obtained from Merck and used without further purification. Xanthone (99%, Aldrich) was recrystallized from ethanol, the triethylamine (TEA, 99%, Aldrich) was distilled under vacuum. Methyl methacrylate (**MMA**, ≥99%, Fluka) was washed with 5% aq. NaOH solution, dried over $CaCl_2$ and distilled in vacuum. The 2-benzoylxanthene was prepared according to the previously described procedure [11a]. The preparations were carried out under argon atmosphere using Schlenk techniques. Melting points were taken on a Büchi 510 apparatus and are uncorrected. Infrared spectra were recorded on a Perkin-Elmer FT-IR Spectrum GX as KBr pellets. ^{1}H and ^{13}C NMR spectra were measured in $CDCl_3$ solutions on a Brucker AC-250 spectrometer. Chemical shifts (δ) are given in ppm and referenced with respect to the residual signals of the solvent, J values in Hz. Mass spectra were measured on an Agilent 1100 Series LC-MSD-Trap-SL spectrometer.

2.2. Synthesis of 2-benzoyl-xanthone (*BzX*)

A hot (∼80 °C) solution of 0.5 g (1.75 mmol) of 2-benzoylxanthene in 2.5 ml acetic acid was added slowly to a stirred hot solution (∼80 °C) of 1.5 g (5.73 mmol) $Na_2Cr_2O_7$ in 5 ml acetic acid. The mixture was heated at 100 °C for 30 min until the oxidation reaction was completed (checked by TLC). The resulting deeply green solution was left to cool and then hydrolyzed. A greenish-yellow crude solid product was isolated and recrystallized from a mixture of ethanol/chloroform (4:1) giving pale yellow crystals (0.33 g, yield 64%); m.p.: 144–145 °C (lit. [11b] m.p.: 146–147 °C); IR (KBr) (cm^{-1}): 3062 (C–H, Ar), 1660 (C=O, xanthone), 1651 (C=O, ketone), 1605 (C=C, Ar), 1464, 1345, 1316, 1277, 1265 (C–O), 1108, 757, 741; ^{1}H NMR ($CDCl_3$, 250 MHz, 298 K) δ (ppm): 8.70 (1H, d, J = 2 Hz, H_1), 8.31 (1H, dd, J = 8.7, 2 Hz, H_3), 8.28 (1H, dd, J = 8.7, 2 Hz, H_4), 7.78 (2H, dd, *ortho*-H), 7.73 (1H, t, *para*-H), 7.70–7.30 (6H, m, $H_{5,6,7,8}$ and *meta*-H); ^{13}C NMR ($CDCl_3$, 68.9 MHz, 298 K) δ (ppm): 194.9 (C=O), 176.6 (C=O), 158.5 (q), 156.0 (q), 137.2 (q), 135.7, 135.3, 133.2 (q), 132.7, 129.9, 128.9, 128.5, 126.8, 124.6, 121.8 (q), 120.9 (q), 118.8, 118.1; MS (APCI$^+$) m/z: 301.2 [M+H]$^+$, MSMS (ESI$^+$) m/z: 223 (M+-Ph) 104.7 [PhCO$^+$].

2.3. Photopolymerization

Photopolymerizations were carried out in Pyrex tubes (λ > 300 nm) containing 3 ml of methylmethacrylate and the proper amounts of initiator and triethylamine. They are filled with dry argon prior to irradiation and are placed in a thermostatic bath. An Osram 400 W high pressure lamp was used as light source. At the end of the irradiation the reaction mixture was poured into excess of cold methanol for precipitation. The polymer was isolated by filtration and drying to constant weight in vacuum. The monomer conversions for all samples were determined gravimetrically.

2.4. UV absorption and fluorescence spectroscopy

Absorption spectra were recorded with a UV-vis Hitachi U-2001 spectrophotometer. Fluorescence and excitation spectra were obtained on a Cary Eclipse fluorescence spectrometer at 25 °C.

2.5. Steady-state UV photolyses

The photolyses were performed with a high pressure mercury lamp (400 W) at 20 °C in quartz cuvettes. The photolysis solutions (∼1 mM) were purged with argon or oxygen before irradiation.

2.6. Electrochemistry

Cyclic voltammetric measurements were carried out using a Metrohm instrument, Model 797 VA, Computerace equipped with a three-electrode cell, containing a hanging mercury drop electrode (HMDE) as a working electrode, a platinum wire as an auxiliary electrode and an Ag/AgCl (3.0 mol L^{-1} KCl) reference electrode. The measurements were performed under a nitrogen atmosphere at 25 °C in acetonitrile (ACN, Merck Uvasol reagent grade) containing

0.1 M $TBAPF_6$ (tetrabutylammonium hexafluorophosphate) as the supporting electrolyte and at scan rate of 0.1 V s^{-1}.

2.7. ns-Laser flash photolysis

Solutions of compounds (A/cm ~ 0.5) were deoxygenated by bubbling with nitrogen or purged with oxygen and were photolysed at 20 °C in a flow system (Suprasil quartz cell) by the fourth harmonics (266 nm) of a Quanta-Ray GCR-11 Nd:YAG laser (Spectra Physics, pulse duration <3 ns) with energies of 0.5–10 mJ. The optical detection system consisted of a pulsed xenon lamp (XBO 150, Osram), a monochromator (Spectra Pro 275, Acton Research Corporation), an R955 photomultiplier tube (Hamamatsu Photonics) or a fast Si-photodiode with 1 GHz amplification, and a 1 GHz digitizing oscilloscope (DSA 684A, Tektronix).

2.8. Quantum yield of triplet formation (Φ_T)

Triplet quantum yield, Φ_T, was determined by energy transfer to perylene acting as triplet energy acceptor (E_T = 147 kJ/mol) [12]. Optical matched MeCN solutions (deaerated) of **BzX**, xanthone (**X**) and benzophenone (**BP**) as reference, were prepared in the presence of identical concentrations of perylene. The concentrations should be high enough to guarantee quantitative quenching of the triplets ^{3}**BzX***, ^{3}**X***, and ^{3}**BP*** created using 266-nm laser light. The quantum yield was calculated by comparing the T–T absorption of the perylene triplet [13] produced by energy transfer from ^{3}**X***, ^{3}**BzX*** and the reference (^{3}**BP***) according to the following equation $\Phi_T(\mathbf{Y}) = \Phi_T(^3\mathbf{BP}^*)\,\Delta A_{TPr}(\mathbf{Y})/\Delta A_{TPr}(^3\mathbf{BP}^*)\,\Phi_T(\mathbf{Y})$ is the triplet quantum yield of ^{3}**BzX*** and ^{3}**X***, while $\Phi_T(^3\mathbf{BP}^*) = 1$ is the reference. $\Delta A_{TPr}(\mathbf{Y})$ and $\Delta A_{TPr}(^3\mathbf{BP}^*)$ are the corresponding absorbance of the perylene triplet at 490 nm after triplet energy transfer from ^{3}**X***, ^{3}**BzX*** and ^{3}**BP***, respectively.

2.9. Measurement of the absorption coefficient (ε_T) of triplet states

2.9.1. Actinometer method

This method is a comparative actinometry method using benzophenone triplet (^{3}**BP***) in acetonitrile as reference [Φ_T(**BP**) = 1, ε_T(**BP**) = 6500 L mol^{-1} cm^{-1} at 520 nm] [14]. Optically matched samples of **BP** and **BzX** were irradiated with the 266 nm laser light in nitrogen-saturated solutions. The triplet state absorbance of **BP** at 520 nm and of target compound **Y** (**BzX** at 540 nm) were measured at different laser intensities. A plot of ΔA_T of **BP** and **BzX** as a function of laser doses [14b] was then used to calculate the absorption coefficient of triplet–triplet absorption [$\boldsymbol{\varepsilon_T}$**(Y)**] of compound according to equation $\varepsilon_T(\mathbf{Y}) = \Phi_T(\mathbf{BP})[\varepsilon_T(\mathbf{BP})\Delta A_T(\mathbf{Y})]/[\Phi_T(\mathbf{Y})\Delta A_T(\mathbf{BP})]$, where ε_T is the triplet molar absorption coefficient of **BP** or **Y**, and ΔA_T(**BP**) and ΔA_T(**Y**) are the slopes of the triplet absorbance versus laser doses for **BP** or **Y**, respectively.

2.9.2. Singlet depletion method

A second method is the singlet depletion technique which is based on the well known relationship $\varepsilon_T = \varepsilon_S\,\Delta OD_T/\Delta OD_S$ [14b] where ΔOD_S is the absorbance of the parent compound (negative signal relative to the baseline) and ΔOD_T that of the triplet state appeared in the transient absorption spectrum. The ε_S was measured from the absorption spectrum. This method requires that no triplet absorption overlaps with the ground state bleach.

2.10. Quantum mechanical calculations

Recent developments of computational chemistry constitute a very useful tool for calculating geometries, energies, vibrational frequencies and other important molecular properties of ground and excited states.

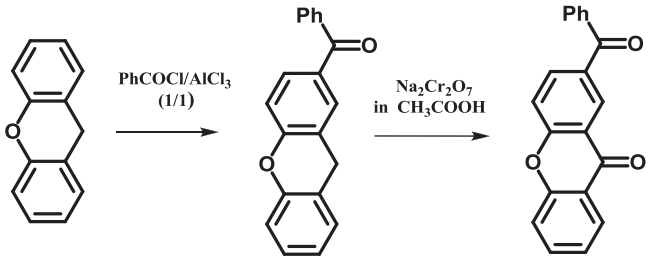

Scheme 2.

Semi-empirical (PM3, AM1), ab initio and DFT calculations were performed using the GAUSSIAN 98 or GAUSSIAN 03 program [15]. The optimized geometry, vibrational modes, and vibrational wavenumbers for the ground-state benzophenone, xanthone, **BzX**, and their triplet states were obtained from DFT/B3LYP calculations (restricted in the case of ground and unrestricted in the case of triplet state and radicals) using the 6-31G(d) basis set. No imaginary wavenumbers were observed at any of the optimized structures shown here. The zero point vibrational energy and enthalpy correction were used without scaling. Time dependent-density functional theory (TD-DFT) calculations were performed to estimate the electronic transition energies and their oscillator strengths.

3. Results and discussion

3.1. Synthesis

The synthesis of **BzX** was performed by a two step reaction procedure (Scheme 2). The first step is a Friedel-Crafts benzoylation of xanthene using benzoyl chloride and $AlCl_3$ as catalyst in CS_2, while the second step concerns a typical oxidation with $Na_2Cr_2O_7$ in CH_3COOH. Their structure were confirmed by ^{1}H and ^{13}C NMR, FT-IR and MS spectra (see Section 2).

3.2. Ground state geometry of *BzX*

Starting with low cost PM3 and AM1 semiempirical calculations we found two different rotamers (**BzX$_{syn}$** and **BzX$_{anti}$**), as expected from the rotation of the benzoyl group. The first one has the two carbonyl groups orientated in the same side of the molecule (**syn**) and the second opposite (**anti**) (Fig. 1). Additionally, each rotamer has an isoenergetic mirror image conformer **BzX***(see Fig. S1, Supplementary material). The optimized geometry of each conformer found by semiempirical calculations (PM3 and AM1) was reoptimized by restricted HF and DFT method with the B3LYP function and 6-31G and 6-31G(d) basis set. The optimized geometric parameters from the DFT calculation (bond lengths and angles) for **BzX** are listed in Supplementary material, Table S1. From the two conformers, the **anti** is predicted to be more stable by about 0.5–1.1 kcal/mol depending on the calculation methodology used (see Table S2, supplementary material). In all cases the xanthone moiety possesses a planar geometry.

3.3. UV–vis spectroscopy and TD-DFT calculations

The UV absorption spectra of **BzX** (Fig. 2) and xanthone **X** (reference compound) were measured in the range of 10^{-3} to 10^{-6} (mol L^{-1}) in MeCN, cyclohexane and MeOH and the values of the molar absorption coefficients (ε) and the wavelength of maximum absorptions (λ_{max}) are summarized in Table S3 (Supplementary Information). The spectra of **X** and **BzX** are similar, except of the ~20 nm red-shift of the more intense band of **X** and **BzX** (from

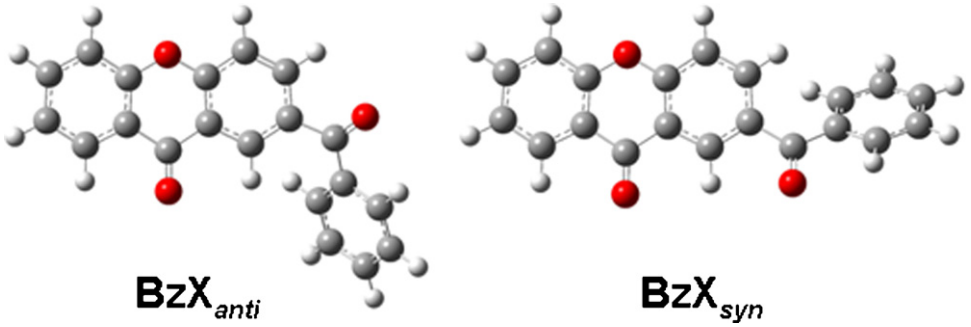

Fig. 1. Optimized ground-state conformations of **BzX** calculated at the DFT/B3LYP/6-31G(d) level.

237 to 255 nm). As the solvent was changed from nonpolar cyclohexane to polar MeCN or MeOH, all absorption bands were slightly shifted toward longer wavelengths and were became broader. This red-shift and the high values of ε is indicative of $\pi \rightarrow \pi^*$ type transitions. The carbonyl n–π^* transition should be expected to occur on the tail of the absorption spectrum (for example in xanthone it appears at ~380 nm), but the low solubility of **BzX** in these solvents prevented its observation.

Extensive spectroscopic as well as theoretical studies have been devoted to xanthone [16–25]. Substitution on the 2-position (e.g., 2-MeO-xanthone) does not change appreciably the basisity and the π-electron density on the carbonyl oxygen and the *ipso*-carbon C2 [18]. We have applied the time dependent density functional theory method (TD-DFT) for **X** and both conformers of **BzX**. This method is able to predict absorption wavelengths corresponding to vertical electronic transitions at a relatively small computer time based on optimized ground state geometries and gives additionally an estimation of the solvent effect [26]. In our case, the TD-DFT method was used with B3LYP and PBE1PBE functions and 6-31G+(d) basis set and the calculations were performed for vacuum/gas phase and in MeCN using the polarized continuum model (CPCM) [27]. The results are presented and compared with experimental data (Fig. 2, and for more detailed results see Supplementary Information, Table S4). The B3LYP function gives better results for the transitions in the area >300 nm, while the PBE1PBE function reproduces the transitions well in <300 nm. In line with literature reports [18], we found very small p-orbital coefficients of the *ipso*-carbon C2 regarding orbitals HOMO-3, HOMO-2, HOMO-1 and LUMO involved in the transitions of **X** and **BzX**. As a consequence, it is not surprising to find little spectral change by introducing the 2-benzoyl group in **BzX** and that the transitions are mostly localized either in the xanthone or the benzoyl part. Characteristic is the HOMO → LUMO transition which is localized on the xanthyl group leaving the phenyl group almost uninvolved (Fig. 3).

While the xanthone molecule shown weak fluorescence spectrum, the emission spectra of **BzX** at room temperature were below

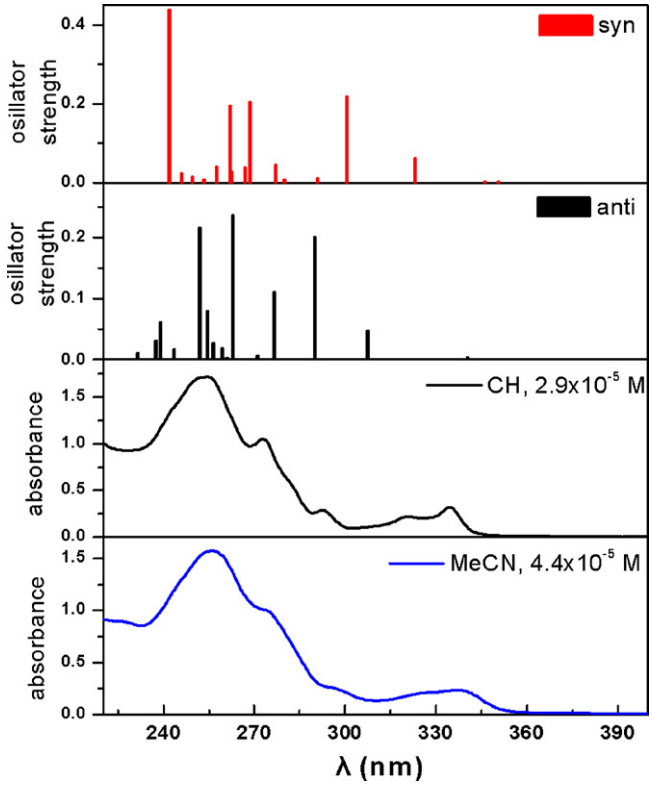

Fig. 2. Absorption spectra of **BzX** in acetonitrile (black line) and cyclohexane (blue line). Electronic transition energies and the corresponding oscillator strengths (gas phase) computed at TD-DFT/PBE1BPE/6-31G+(d) on the optimized DFT/B3LYP/631G(d) ground state geometry (syn- and anti-rotamer). (For interpretation of the references to colour in this figure legend, the reader is referred to the web version of the article.)

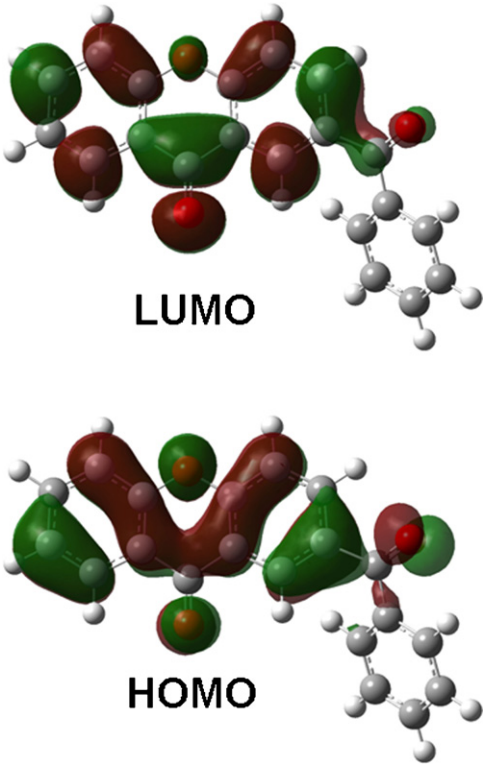

Fig. 3. Calculated unoccupied (LUMO) and occupied (HOMO) molecular orbitals of the anti rotamer of **BzX** at the B3LYP/6-31G+d level of theory.

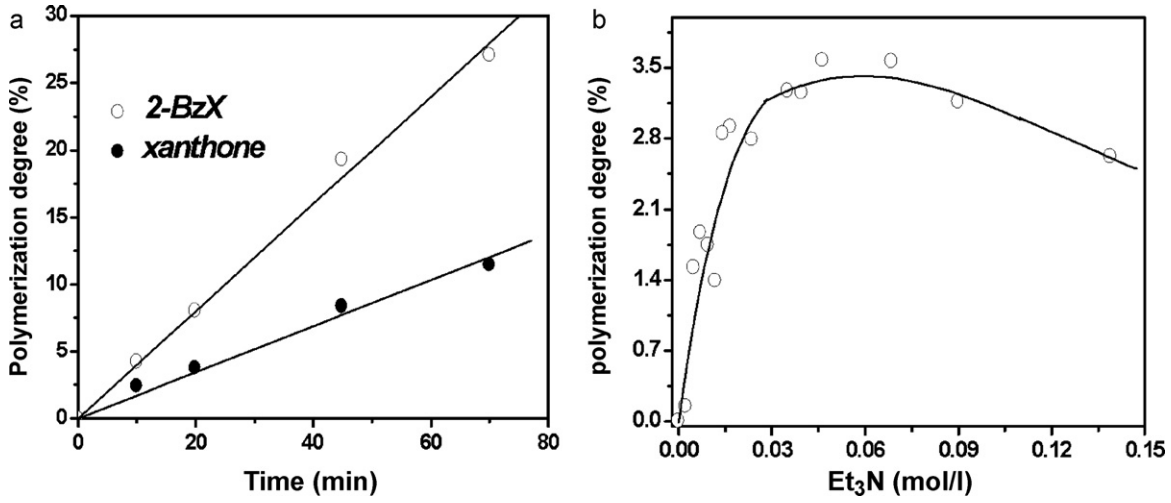

Fig. 4. (a) Time conversion curves for the bulk polymerization of MMA (9.42 mol L^{-1}) at 30 °C using **BzX** or **X** as photoinitiator (5×10^{-3} mol L^{-1}) and **Et_3N** (0.1 mol L^{-1}) as co-initiator; (b) polymerization yield (%) as a function of **Et_3N** concentration at 25 °C after 10 min irradiation using **BzX** as photoinitiator (5×10^{-3} mol L^{-1}).

the detection limit of the conventional fluorescence spectrometer used in the solvents like cyclohexane and MeCN.

3.4. Photopolymerization reaction

Polymerization was performed by irradiating a bulk solution of **BzX** or **X** in **MMA**. Fig. 4a shows the time conversion curves of the **MMA** polymerization using either **X** or **BzX** as photoinitiators with **Et_3N** as co-initiator at 30 °C. It is apparent that the polymerization yield in both cases are increases linearly with the time, while the polymerization rate (R_p), determined from the slopes of the straight lines is more than two times greater in the case of **BzX** initiator (Table 1). The dependence of the polymerization yield with triethylamine concentration after 10 min irradiation at 25 °C is shown in Fig. 4b. The photoinitiation efficiency increases with the amine concentration, reaching an optimum value at 0.02–0.1 M.

3.5. Nanosecond laser flash photolysis

3.5.1. Properties of the triplet state of *BzX*

Photoexcitation of a deoxygenated solution of **BzX** in acetonitrile with 266-nm (or 355-nm) laser light resulted in the formation of a transient absorption signal with maxima at 325, 355, 530 nm and a shoulder at ~610 nm (Fig. 5, top) which we attribute to the triplet state of **BzX** (^{3}**BzX***), see below. Additionally, a strong negative band (depletion of parent compound) appeared at wavelength <300 nm with minimum at 260 nm (see Fig. 5 bottom). The decay of transient signal can be fitted with first-order kinetics (see insets in Fig. 5 top) at low excitation doses and has a lifetime of 22.7 μs. An identical value was obtained also for the negative signal, a fact indicating that the decay of the triplet leads to the regeneration of the parent compound. The existence of an isosbestic point at 290 nm supports further this suggestion. The linear dependence of the absorption of this transient versus laser doses indicates that their formation is a monophotonic process (Fig. 5 top, inset). At higher excitation doses, the decay becomes faster and involves as expected a second-order component as a result of triplet–triplet annihilation.

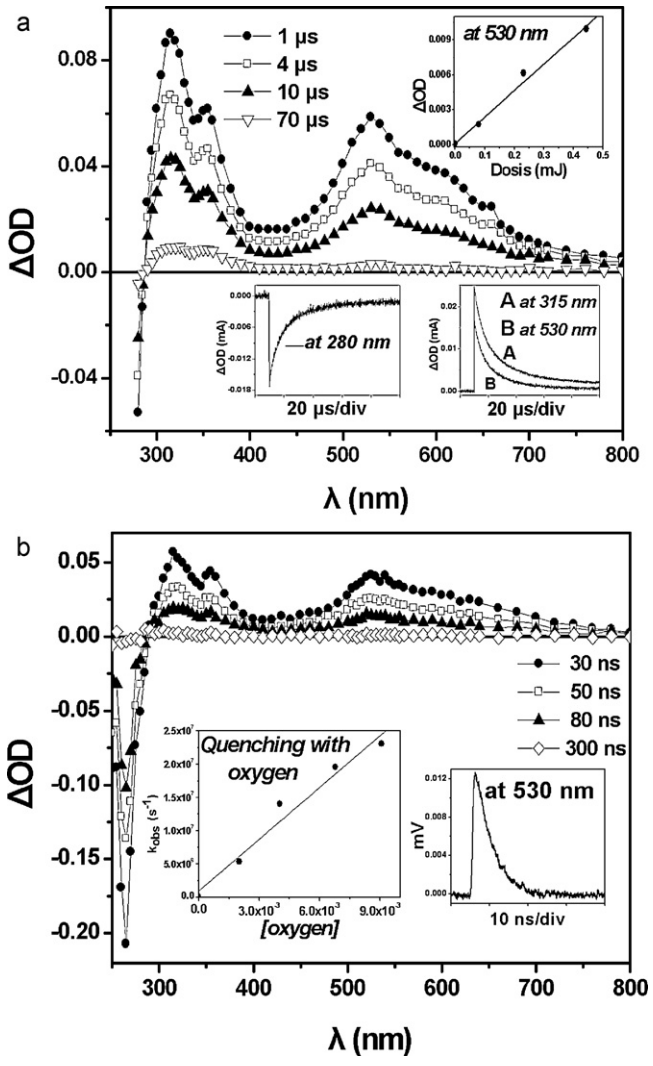

Fig. 5. Transient absorption spectra recorded after 266-nm laser excitation of **BzX** in acetonitrile; in nitrogen saturated solution (top) and in oxygen saturated solution (bottom). Inset (top): time profiles at 280 nm (recovery of ground state), at 315 and 530 nm and the photonity plot at 530 nm. Inset (bottom): decay at 530 nm and quenching plot with oxygen.

Table 1
Photopolymerization of **MMA** with **BzX** in bulk at 30 °C.

[Initiator] (mol L^{-1})	[TEA] (mol L^{-1})	R_p ($\times 10^4$ mol L^{-1} s^{-1})
X	0.1	3.04
BzX	0.1	7.06

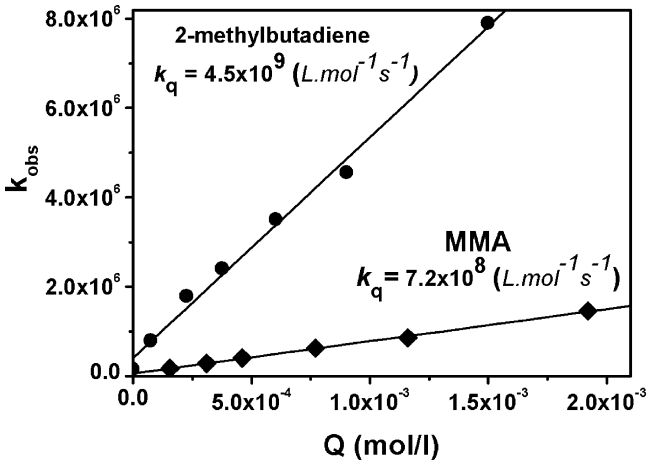

Fig. 6. Quenching of **BzX** triplet at 530 nm by 2-methylbutadiene and **MMA** in deaerated acetonitrile solution.

Under an oxygen atmosphere exactly the same transient was recorded (Fig. 5 bottom), but its decay is accelerated following pseudo first-order kinetics with a value of $k_{obs} = 2.2 \times 10^7\ s^{-1}$. By taking into account the concentration of oxygen in MeCN at room temperature ($[O_2] = 9.1$ mM [12]), a bimolecular rate constant of $2.4 \times 10^9\ L\,mol^{-1}\,s^{-1}$ is evaluated, close to the quenching rate constant of triplet xanthone ($5.6 \times 10^9\ L\,mol^{-1}\,s^{-1}$ in benzene) [30a] or triplet benzophenone with oxygen ($2.3 \times 10^9\ L\,mol^{-1}\,s^{-1}$) [28], see the inset in Fig. 5 bottom.

Further evidence characterizing this transient as triplet ^{3}**BzX*** is derived from its quenching with typical triplet quenchers like 2-methylbutadiene (isoprene) with $E_T = 60$ kcal/mol [29], perylene ($E_T = 35.1$ kcal/mol [12]) and **MMA**. We found typical quenching rate constants $k_q = 4.5 \times 10^9\ L\,mol^{-1}\,s^{-1}$ (2-methylbutadiene), $1.0 \times 10^{10}\ L\,mol^{-1}\,s^{-1}$ (perylene) and $7.2 \times 10^8\ L\,mol^{-1}\,s^{-1}$ (**MMA**). In Fig. 6 we show a representative quenching plot using the equation $k_{obs} = k_o + k_q[Q]$, where k_o is the first order rate constant for triplet decay in the absence of quencher Q.

Comparison of the absorption spectra of ^{3}**BzX*** with that of xanthone triplet (^{3}**X***) shows that they are much different; ^{3}**X*** has been reported to show a maximum at about 630 nm in acetonitrile [30a–k], see Table 3 for more details. On the contrary, the bands observed for ^{3}**BzX*** are almost similar to the corresponding spectrum of benzophenone triplet (^{3}**BP***) or its derivatives and this is a first indication that the triplet excitation is localized mostly on the benzoyl substituent and less to the xanthone moiety. This assumption is further supported by the computational results reported (Section 3.5.2).

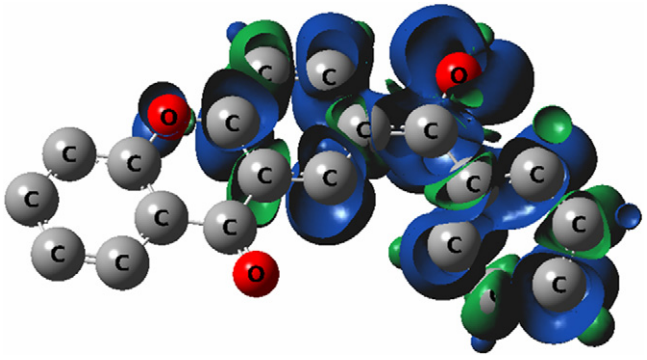

Fig. 8. Spin density distribution of triplet ^{3}**BzX*** (anti rotamer).

3.5.2. Triplet state geometry and energy calculations

As already shown (Section 3.2) **BzX** exhibits two different rotamers (***syn*** and ***anti***). The triplet states of the two rotamers are optimized at the unrestricted DFT/B3LYP/6-31G(d) level. Although the optimized geometry of ^{3}**BzX*** remains similar to the corresponding ground state (see Fig. 7), there are substantial geometrical changes located around the carbonyl group (C16–O17) of the benzoyl substituent (see details in Table S1, Supplementary material). The comparison reveals that the benzoyl carbonyl bond is lengthened by about 0.1 Å, while the C2–C16 and C16–C18 bonds are shortened by about 0.056 and 0.051 Å, respectively. Additionally, the Mulliken atomic charges (Table 2) increase from −0.471 (ground state) to −0.330 (triplet state) on the oxygen (O17) and decrease from 0.324 to 0.213 on the carbon atom (C16). On the same time the spin density resides almost exclusively in the benzoyl group, e.g. 0.938 (O17) versus −0.003 (O11), see Fig. 8 and Table 2. In contrast, geometry and charges of the xanthenyl carbonyl C9–O11 group remain almost unchanged. The above findings show the existence of an n→π* triplet state (^{3}**BzX***) localized on the benzoyl group in agreement with the laser experiments and the localized character of the transitions described above.

We calculated with B3LYP/6-31G(d) the triplet energies of ^{3}**BzX***, ^{3}**X*** and ^{3}**BP*** using relaxed ground and triplet state geometries and added ZPE corrections. We found 62.0 kcal/mol for the ***anti*** and 61.1 kcal/mol for the ***syn*** conformer of ^{3}**BzX***, 68.3 kcal/mol for ^{3}**X*** (experimental value 74.1 kcal/mol [28]) and 61.6 kcal/mol for ^{3}**BP*** (experimental value 68.6 kcal/mol [28]). The energy of ^{3}**BzX*** is closer to benzophenone than to xanthone, corroborating hitherto met conclusions for the localization of triplet excitation in the benzoyl chromophores (see Table 3).

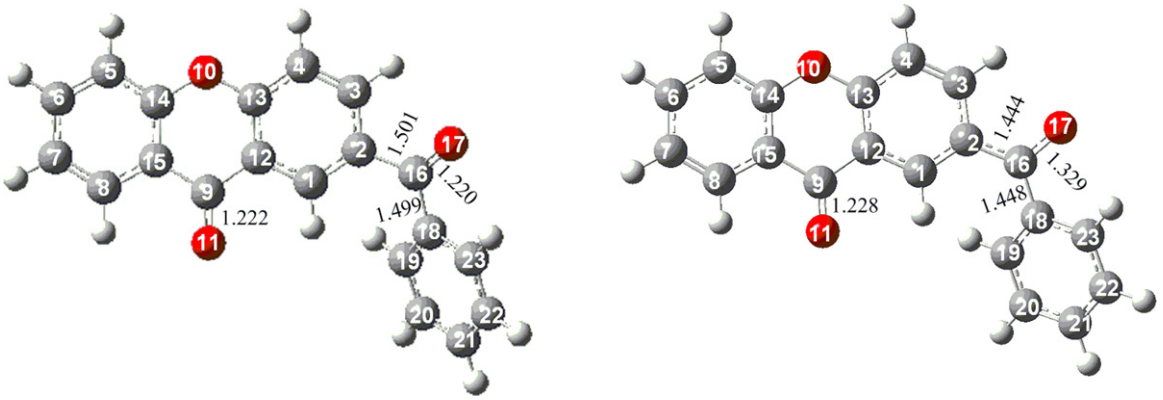

Fig. 7. Optimized geometries of **BzX** (left) and ^{3}**BzX*** (right) of the anti rotamer.

Table 2
Mulliken atomic charges in ground state, triplet state and triplet state spin densities of **BzX**, calculated at the B3LYP/6-31G(d) level.

Atom	Ground state	Triplet state	Triplet spin density	Atom	Ground state	Triplet state	Triplet spin density
C1	−0.239	−0.252	0.1893	C13	0.309	0.297	0.1458
C2	0.071	0.105	−0.0447	C14	0.298	0.299	−0.0021
C3	−0.150	−0.170	0.1348	C15	0.061	0.058	0.0075
C4	−0.187	−0.184	−0.0821	C16	0.324	0.213	0.4426
C5	−0.182	−0.183	0.0039	O17	−0.471	−0.330	0.9384
C6	−0.127	−0.127	0.0001	C18	0.075	0.100	−0.0210
C7	−0.134	−0.135	0.0056	C19	−0.173	−0.171	0.1374
C8	−0.172	−0.172	0.0005	C20	−0.135	−0.135	−0.0605
C9	0.383	0.381	0.0067	C21	−0.118	−0.125	0.1976
O10	−0.552	−0.551	−0.0027	C22	−0.135	−0.132	−0.0934
O11	−0.506	−0.506	0.0134	C23	−0.150	−0.155	0.1745
C12	0.055	0.063	−0.0619				

3.5.3. Determination of triplet state quantum yield and ε_T

Triplet state quantum yields were determined by using the triplet energy transfer method to perylene. Perylene shows triplet energy of 147 kJ/mol [13] and has a very low intersystem crossing quantum yield ($\Phi_{ISC} = 0.011$). Thus, perylene triplet can only be formed through energy transfer from a suitable triplet donor. Since perylene has a characteristic triplet–triplet absorption showing a sharp peak at 490 nm, the quenching process could be easily monitored either by following the triplet decay (^{3}**X*** at 630 nm, ^{3}**BP*** at 520 nm, and ^{3}**BzX*** at 530 nm), or following the exponential growth of the perylene triplet at 490 nm (see Fig. S4 in Supplementary material). Due to high triplet energy differences between the donor and acceptor, a diffusion-controlled rate constant was found for the triplet energy transfer of **BzX**: $k_q \sim 1.0 \times 10^{10}$ L mol^{-1} s^{-1} in MeCN, a fact which further confirms the triplet nature of the transient obtained upon laser excitation of **BzX** (Fig. 5). Using **BP** as standard ($\Phi_T = 1$), a value of $\Phi_T = 0.97$ was found for xanthone identical to the bibliographic value in CCl_4 [30c]. For the **BzX** a value of 0.78 and 0.81 was obtained using the 266 and 355 nm laser excitation respectively, see Table 3.

The triplet absorption coefficient of **BzX** at 530 nm was calculated with two different methodologies (see Section 2): the singlet depletion methodology gave a value of 7900 L mol^{-1} cm^{-1} and using benzophenone as actinometer a value of 7500 L mol^{-1} cm^{-1} was found.

3.5.4. The reaction of *BzX* triplet with *Et_3N* and formation of ketyl radical

Fig. 9 shows the transient absorption spectrum obtained after 266-nm laser excitation of the system **BzX**/**Et_3N** in acetonitrile at 295 K (an analogous spectrum with 355-nm laser light was depicted in Fig. S5 of Supplementary Material). The signal originally obtained (80 ns after the pulse) is almost similar to the triplet state absorption (Fig. 4), and was later replaced (3 μs) by a different spectrum showing maxima at 345 nm (with a shoulder at ∼330 nm) and 540 nm. The transient decays with first order-kinetics measured at 620 nm ($k_{obs} = 1.8 \times 10^6$ s^{-1}) and is followed by the build up of the ketyl radical spectrum with maxima at 345 ($k_{obs} = 1.9 \times 10^6$ s^{-1}) and 540 nm respectively (see the inset of Fig. 9). The ketyl radical is the well-known photoreduction product of carbonyl triplet [42], while the expected *a*-aminoethyl radical (•CHMe-NEt_2) is not visible under our experimental conditions.

We produced the ketyl radical following a different path, by irradiating a solution of **BzX** in cyclohexane (Fig. 10). The spectrum recorded immediately after the laser pulse is similar to the spectrum of the triplet state in MeCN and changes later (850 ns) to a new transient which we attribute to the ketyl radical of **BzX** being almost identical with that observed with **Et_3N** in MeCN (3 μs, Fig. 9). The decay of **BzX** ketyl radical at later time domain (second order) and in oxygen atmosphere is presented at Supplementary Material Fig. S6 and Fig. S7. The spectral characteristics of the **BzX** ketyl rad-

Table 3
Spectral characteristics of the triplet states (absorption maxima in MeCN and cyclohexane, lifetimes, quantum yields, $T_n \leftarrow T_1$ extinction coefficient and triplet energies) of xanthone (**X**), benzophenone (**BP**) and **BzX**.

Compound	λ_{max} $T_n \leftarrow T_1$[a] (nm)		$\tau_{triplet}$ (μs)		Φ_T	ε of $T_n \leftarrow T_1$ (L mol^{-1} cm^{-1})	E_T (kcal/mol)
	MeCN	CH	MeCN	CH	MECN		
X	635	610		0.02	0.90[d]	5300[b]	74.1[g]
	620				0.97[f]	8600[c]	73[d]
	630		16.8			9500[d]	72[o]
	631		8.3	0.022			
	627		0.95				
BP	520	535	14 μs	0.3[n]	1	6500[e]	68.6 and 69.2[i]
BzX	315	315	22.7	0.105	0.78[j]	7500[l]	68.5[o]
	355	340			0.81[k]	7900[m]	
	530	530					

[a] Ref. [30a–k].
[b] In benzene Ref. [30a].
[c] In benzene Ref. [34].
[d] In EtOAc Ref. [35].
[e] In MeCN Ref. [14].
[f] In CCl_4 Ref. [30e].
[g] Refs. [17,36,37].
[i] Ref. [12], p.107.
[j] With 266 nm excitation laser light.
[k] With 355 nm excitation laser light.
[l] **BP** actinometry.
[m] Singlet depletion.
[n] Ref. [41].
[o] $T_1 \leftarrow S_o$ from TDDFT calculations (see text).

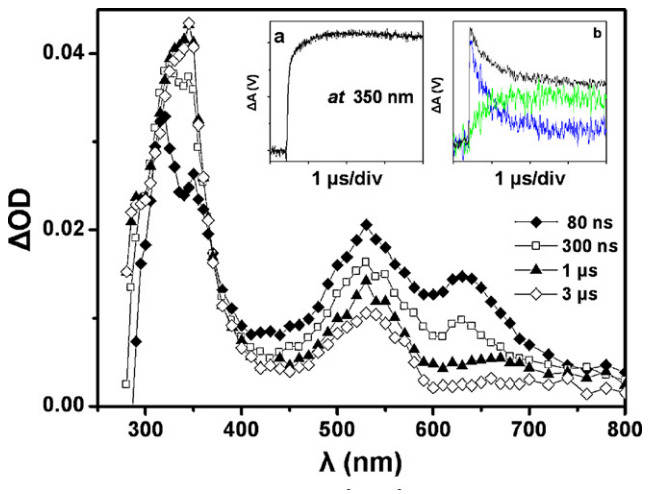

Fig. 9. Transient absorption spectra observed in the laser photolysis of **BzX** (1.35×10^{-5} mol L^{-1}) and **Et_3N** (2.9×10^{-4} mol L^{-1}) with 266 nm laser light in nitrogen saturated MeCN; (♦) 80 ns, (□) 300 ns, (▲)1.50 μs and (◊) 3.0 μs after the laser pulse. Inset: (a) the build up of ketyl radical at 350 nm and (b) normalized decay profiles at 540 (black line), at 620 nm (blue line) and the simulated build up of ketyl radical at 540 nm (green line). (For interpretation of the references to colour in this figure legend, the reader is referred to the web version of the article.)

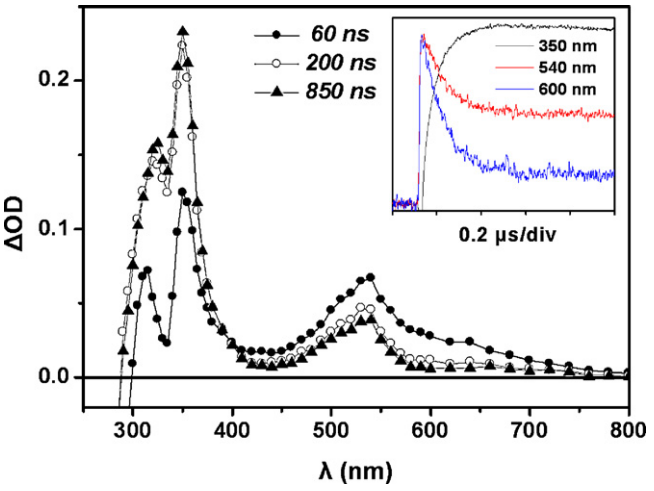

Fig. 10. Transient absorption spectra recorded after 266 nm laser excitation of **BzX** in cyclohexane solution at (●) 60 ns, (○) 200 ns and (▲) 850 ns after the laser pulse. Inset: decay at 600 (blue line) and 540 nm (red line) and the build up of ketyl radical at 350 nm (black line) with normalized amplitude. (For interpretation of the references to colour in this figure legend, the reader is referred to the web version of the article.)

ical are similar to the benzophenone ketyl radical but differ from the xanthone ketyl; the latter has a maximum at about 450 nm and a broad absorption which extends until 800 nm [30a,e,g,k] which is absent in **BzX** ketyl. Supportive evidence comes from open-shell DFT/B3LYP/6-31G(d) calculations which showed that the benzoyl ketyl type radical (**I**) is more stable than the xanthyl ketyl radical (**II**) by about 3 kcal/mol (Scheme 3).

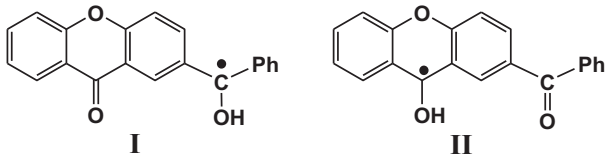

Scheme 3.

The above characteristics reflect the n–π* character of **BzX** triplet, in agreement with the TD-DFT calculations for the $S_o \rightarrow T_1$ transition which takes place at 415.6 nm in the gas phase and at 401.7 nm in MeCN; this blue shift supports further the n–π* character of the transition.

The bimolecular quenching rate constant of **^{3}BzX*** with **Et_3N** (electron transfer) in MeCN was measured, $k_q = 3.5 \times 10^9$ L mol^{-1} s^{-1} (Fig. S9 of Supplementary Material) and was found to be very close to corresponding literature values of **^{3}BP*** ($k_q = 3.5 \times 10^9$ L mol^{-1} s^{-1} [39] and 4.0×10^9 L mol^{-1} s^{-1} [40] respectively). A slightly greater value was reported in the case of **^{3}X*** in the same solvent ($k_q = 4.4 \times 10^9$ L mol^{-1} s^{-1} [39] and 2.4×10^9 L mol^{-1} s^{-1} [30k]). The observed values are in accordance to the free energy values (**ΔG_{et}**) which are obtained applying the Rehm–Weller equation [31] and using the measured redox potentials of the **X** and **BzX** and literature values of **X** and **BP** [32,33]. A free energy value (ΔG_{et}) of −10.6 kcal/mol was obtained for the electron transfer from NEt_3 to **^{3}BzX*** and a value of −13.8 kcal/mol for the **^{3}X*** (see the electrochemical details in Supplementary Material).

3.5.5. Conclusions

The present investigation shows that introduction of the benzoyl group in xanthone (**X**) produces the 2-benzoyl xanthone (**BzX**) which enhances the photoinitiator activity of methylmethacrylate (**MMA**) using **Et_3N** as co-initiator (Table 1). The spectroscopic and theoretical results presented above, indicate a type-**II** photoinitiation system which follows the typical mechanistic scheme for the photoreduction of aromatic ketones by amines, as has been established by numerous studies [42]. Thus, after excitation in polar solvents like acetonitrile, a contact ion pair (CIP) was formed *via* electron transfer between the triplet **^{3}BzX*** and **Et_3N** (Scheme 4, **a**). This triplet contact ion pair follows three possible decay pathways: to undergo proton transfer generating a triplet radical pair (ketyl and α-aminoethyl radical, pathway **b**), to form a solvent separated ion pair (SSIP, step **c**), or to undergo back-electron transfer regenerating the reactants (step **d**). The resulting α-aminoethyl radical initiates finally the polymerization of the monomer **MMA**.

Upon excitation of **BzX** with the 266 nm or 355 nm laser light in MeCN solvent, the triplet state **^{3}BzX*** was produced and the quantum yield ($\Phi = 0.80$) and its molar absorption coefficient was determined. Based on, (i) the spectral characteristics of the transient spectrum (Fig. 5, Section 3.5.1), (ii) the quenching rate constants measured with typical triplet quenchers (Section 3.5.3, Fig. 6), (iii) the observed photoreduction with **Et_3N** (Section 3.5.4) and the reduction potentials determined hereupon (Supplementary Material), as well as (iv) the TD-DFT calculations (Section 3.5.2), it was concluded that **^{3}BzX*** corresponds to an $n \rightarrow \pi^*$ transition localized almost exclusively on the benzoyl substituent; the close similarity to the benzophenone triplet **^{3}BP*** and the disparity from **^{3}X*** strengthens this conclusion further. In other words, the two subunits xanthonyl and benzoyl seem to function as localized chromophores, and, irrespective of which chromophore is originally excited, the lower energy triplet state is finally populated through intramolecular energy transfer. Latter is facilitated through the ca. 6 kcal/mol reduction of the triplet energy of **^{3}BzX*** (being similar to **^{3}BP***) compared to **^{3}X*** (Section 3.5.2).

Obviously, it is just this triplet character and the localization on the benzoyl group which doubles the photoinitiation activity of **BzX** compared to **X** (Table 1) and despite the more favourable driving force (more exergonic ΔG_{et}) of the primary electron transfer event (step **a**, Scheme 4) for the latter (**X**). The reason seems to be the fact that the monomer (**MMA**) functions as a quencher for triplet states: it is much more effective for **^{3}X*** ($k_q = 1.2 \times 10^{10}$ L mol^{-1} s^{-1} [10b]) than for **^{3}BzX*** ($k_q = 7.2 \times 10^8$ L mol^{-1} s^{-1}, see Section 3.5.1). For comparison, the quenching of benzophenone triplet

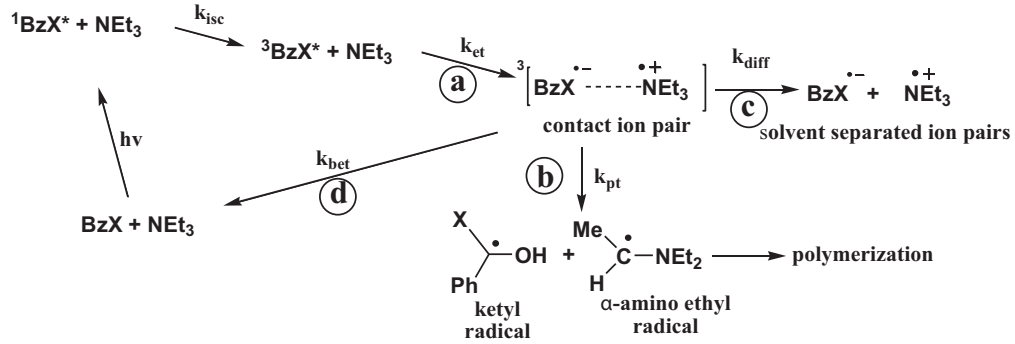

Scheme 4.

^{3}BP* by **MMA** ($k_q = 5.4 \times 10^7$ L mol^{-1} s^{-1} in MeCN [10b] and $k_q = 6.9 \times 10^7$ L mol^{-1} s^{-1} in benzene [38]) was found to be close to that of **^{3}BzX***. In contrast, the quenching with **Et_3N** (the primary electron transfer step **a**), does not differentiate much for **^{3}X*** ($k_q = 4.4 \times 10^9$ L mol^{-1} s^{-1} [39] and 2.4×10^9 L mol^{-1} s^{-1} [30k] in MeCN), for **^{3}BzX*** ($k_q = 3.5 \times 10^9$ L mol^{-1} s^{-1}, Section 3.5.4 and Fig. S9 of Supplementary Material) or for **^{3}BP*** ($k_q = 3.5 \times 10^9$ L mol^{-1} s^{-1} [39], 4.0×10^9 L mol^{-1} s^{-1} [40] in MeCN). Thus, the quenching of xanthone triplet by **MMA** is a very competitive process compared to the crucial electron/proton transfer reaction which affords the desired α-aminoethyl radical through steps **a** and **b**. On the contrary, the electron transfer is more competitive in the cases of **^{3}BzX*** and **^{3}BP***.

Summarizing, the above results show that triplet **^{3}BzX*** behaves like the benzophenone triplet **^{3}BP*** and deviates from that of xanthone **^{3}X***, i.e., triplet excitation is localized mostly on the benzoyl subunit of **BzX**. This property renders 2-benzoyl-xanthone a much more effective type-**II** photoinitiator than the unsubstituted xanthone.

Appendix A. Supplementary data

Supplementary data associated with this article can be found, in the online version, at doi:10.1016/j.jphotochem.2011.02.028.

References

[1] X. Asvos, PhD thesis in preparation, University of Ioannina, Greece.
[2] (a) J.P. Fouassier, J.F. Rabek (Eds.), Radiation Curing in Polymer Science and Technology, vols. I–IV, Elsevier Applied Science, London, 1993;
(b) J.P. Fouassier, Photoinitiation, Photopolymerization and Photocuring Fundamentals and Applications, Hanser Publishers, New York, 1995 (Chapter 1).
[3] C.N. Bowman, C.J. Kloxin, AIChE J. 58 (2008) 2775–2795.
[4] H.F. Gruber, Prog. Polym. Sci. 17 (1992) 953–1044.
[5] A.B. Scranton, C.N. Bowman, R.W. Peiffer (Eds.), Photopolymerization Fundamentals and Applications, ACS, Washington, 1997, ACS Symposium Series 673K.
[6] W. Rutsch, K. Dietliker, D. Leppard, M. Köhler, L. Misev, U. Kolczak, G. Rist, Prog. Org. Coat. 27 (1996) 227–239.
[7] J.P. Fouassier, X. Allonas, D. Burget, Prog. Org. Coat. 47 (2003) 6–36.
[8] R.S. Davidson, A.A. Dias, D. Illsley, J. Photochem. Photobiol. A: Chem. 89 (1995) 75–87.
[9] D.A. Tasis, M.G. Siskos, A.K. Zarkadis, Macromol. Chem. Phys. 199 (1998) 1981–1987.
[10] (a) N.S. Allen, N.G. Salleh, M. Edge, T. Corrales, M. Shah, F. Catalina, W.A. Green, Eur. Polym. J. 33 (1997) 1639–1643;
(b) H.J. Timpe, K.P. Kronfeld, J. Photochem. Photobiol. A: Chem. 46 (1989) 253–267;
(c) H.J. Timpe, K.P. Kronfeld, U. Lammel, J.P. Fouassier, D.J. Lougnot, J. Photochem. Photobiol. A: Chem. 52 (1990) 111–122;
(d) L. Cokbaglan, N. Arsu, Y. Yagci, S. Jockusch, N.J. Turro, Macromolecules 36 (2003) 2649–2653;
(e) G. Temel, N. Arsu, J. Photochem. Photobiol. A: Chem. 202 (2009) 63–66;
(f) M. Aydin, N. Arsu, Y. Yagci, Macromol. Rapid Commun. 24 (2003) 718–723;
(g) M. Aydin, N. Arsu, Y. Yagci, S. Jockusch, N.J. Turro, Macromolecules 38 (2005) 4133–4138.
[11] (a) V. Georgakilas, G.P. Perdikomatis, A.S. Triantafyllou, M.G. Siskos, A.K. Zarkadis, Tetrahedron 58 (2002) 2441–2447;
(b) J. Heller, St. v. Kostanecki, Ber. Dtsch. Chem. Ges. 41 (1908) 1324–1327.
[12] S.L. Murov, I. Carmichael, G.L. Hug, Carmichael, Handbook of Photochemistry, 2nd ed., Marcel Dekker, New York, 1993, p. 57.
[13] (a) S.A. Yamamoto, K. Kikuchi, H. Kokubun, J. Photochem. 7 (1977) 177–184;
(b) R.V. Bensasson, E.J. Land, Trans. Faraday Soc. 67 (1971) 1904–1915.
[14] (a) R.V. Bensasson, J.C. Gramain, J. Chem. Soc., Faraday Trans. 176 (1980) 1801–1810;
(b) I. Carmichael, G.L. Hug, J. Phys. Chem. Ref. Data 15 (1986) 1–250.
[15] (a) M.J. Frisch, G.W. Trucks, H.B. Schlegel, G.E. Scuseria, M.A. Robb, J.R. Cheeseman, V.G. Zakrzewski, J.A. Montgomery Jr., R.E. Stratmann, J.C. Burant, S. Dapprich, J.M. Millam, A.D. Daniels, K.N. Kudin, M.C. Strain, O. Farkas, J. Tomasi, V. Barone, M. Cossi, R. Cammi, B. Mennucci, C. Pomelli, C. Adamo, S. Clifford, J. Ochterski, G.A. Petersson, P.Y. Ayala, Q. Cui, K. Morokuma, D.K. Malick, A.D. Rabuck, K. Raghavachari, J.B. Foresman, J. Cioslowski, J.V. Ortiz, B.B. Stefanov, G. Liu, A. Liashenko, P. Piskorz, I. Komaromi, R. Gomperts, R.L. Martin, M. Challacombe, P.M.W. Gill, B. Johnson, W. Chen, M.W. Wong, J.L. Andres, C. Gonzalez, M. Head-Gordon, E.S. Replogle, J.A. Pople, Gaussian 98 Revision A.9, Gaussian, Inc, Pittsburgh, PA, 1998;
(b) M.J. Frisch, G.W. Trucks, H.B. Schlegel, G.E. Scuseria, M.A. Robb, J.R. Cheeseman, J.A. Montgomery Jr., T. Vreven, K.N. Kudin, J.C. Burant, J.M. Millam, S.S. Iyengar, J. Tomasi, V. Barone, B. Mennucci, M. Cossi, G. Scalmani, N. Rega, G.A. Petersson, H. Nakatsuji, M. Hada, M. Ehara, K. Toyota, R. Fukuda, J. Hasegawa, M. Ishida, T. Nakajima, Y. Honda, O. Kitao, H. Nakai, M. Klene, X. Li, J.E. Knox, H.P. Hratchian, J.B. Cross, V. Bakken, C. Adamo, J. Jaramillo, R. Gomperts, R.E. Stratmann, O. Yazyev, A.J. Austin, R. Cammi, C. Pomelli, J.W. Ochterski, P.Y. Ayala, K. Morokuma, G.A. Voth, P. Salvador, J.J. Dannenberg, V.G. Zakrzewski, S. Dapprich, A.D. Daniels, M.C. Strain, O. Farkas, D.K. Malick, A.D. Rabuck, K. Raghavachari, J.B. Foresman, J.V. Ortiz, Q. Cui, A.G. Baboul, S. Clifford, J. Cioslowski, B.B. Stefanov, G. Liu, A. Liashenko, P. Piskorz, I. Komaromi, R.L. Martin, D.J. Fox, T. Keith, M.A. Al-Laham, C.Y. Peng, A. Nanayakkara, M. Challacombe, P.M.W. Gill, B. Johnson, W. Chen, M.W. Wong, C. Gonzalez, J.A. Pople, Gaussian 03 Revision D.01, Gaussian, Inc., Wallingford, CT, 2004.
[16] F. Scigalski, J. Paczkowski, Macromol. Chem. Phys. 209 (2008) 1872–1880.
[17] (a) H.J. Pownall, J.R. Huber, J. Am. Chem. Soc. 93 (1971) 6429–6436;
(b) H.J. Pownall, R.E. Connor, J.R. Huber, Chem. Phys. Lett. 22 (1973) 403–405.
[18] K. Mizutani, K. Miyazaki, K. Ishigaki, H. Hosoya, Bull. Chem. Soc. Jpn. 47 (1974) 1596–1603.
[19] A.A. Efimov, R.N. Nurmukhametov, I.L. Belaits, A.I. Tolmachev, Opt. Spectrosc. 30 (1971) 337.
[20] T. Minegishi, T. Hoshi, H. Hiratsuka, Y. Tanizaki, Bull. Chem. Soc. Jpn. 50 (1977) 3140–3143.
[21] R.E. Connors, R.J. Sweeney, F. Cerio, J. Phys. Chem. 91 (1987) 819–822.
[22] S. Ishijima, M. Higashi, H. Yamaguchi, J. Phys. Chem. 98 (1994) 10432–10435.
[23] S.L. Zheng, P. Coppens, Chem. Eur. J. 11 (2005) 3583–3590.
[24] A. Thöny, M.J. Rossi, J. Photochem. Photobiol. A: Chem. 104 (1997) 25–33.
[25] B. Heinz, B. Schmidt, C. Root, H. Satzger, F. Milota, B. Fierz, T. Kiefhaber, W. Zintha, P. Gilch, Phys. Chem. Chem. Phys. 8 (2006) 3432–3439.
[26] (a) M. Cossi, V. Barone, J. Chem. Phys. 115 (2001) 4708–4717;
(b) D. Jacquemin, J. Preat, E.A. Perpete, Chem. Phys. Lett. 410 (2005) 254–259;
(c) D. Jacquemin, J. Preat, M. Charlot, V. Wathelet, J.M. Andre, E.A. Perpete, J. Chem. Phys. 121 (2004) 1736–1743.
[27] (a) S. Miertus, E. Scrocco, J. Tomasi, Chem. Phys. 55 (1981) 117–129;
(b) S. Miertus, J. Tomasi, Chem. Phys. 65 (1982) 239–241;
(c) B. Mennucci, E. Cances, J. Tomasi, J. Phys. Chem. 101 (1997) 10506–10517;
(d) M. Cossi, V. Barone, J. Cammi, Chem. Phys. Lett. 255 (1996) 327–335.
[28] S.K. Chattopadhyay, C.V. Kumar, P.K. Das, J. Photochem. 30 (1985) 81–91.
[29] R.E. Kellogg, W.T. Simpson, J. Am. Chem. Soc. 87 (1965) 4230–4234.
[30] (a) A. Garner, F. Wilkinson, J. Chem. Soc., Faraday Trans. 2 (72) (1976) 1010–1020;
(b) F. Wilkinson, A. Garner, J. Chem. Soc., Faraday Trans. 2 (73) (1977) 222–223;
(c) F. Wilkinson, A. Garner, Photochem. Photobiol. 27 (1978) 659–670;
(d) C. Ley, F. Morlet-Savary, J.P. Fouassier, P. Jacques, J. Photochem. Photobiol. A: Chem. 137 (2000) 87–92;
(e) J.C. Scaiano, J. Am. Chem. Soc. 102 (1980) 7747–7753;

(f) C.H. Evans, N. Prud'Homme, M. King, J.C. Scaiano, J. Photochem. Photobiol. A: Chem. 121 (1999) 105–110;
(g) C. Coenjarts, J.C. Scaiano, J. Am. Chem. Soc. 122 (2000) 3635–3641;
(h) H. Satzger, B. Schmidt, C. Root, W. Zinth, B. Fierz, F. Krieger, T. Kiefhaber, P. Gilch, J. Phys. Chem. A 108 (2004) 10072–10079;
(j) K.A. Abdullah, T.J. Kemp, J. Photochem. 32 (1986) 49–57;
(k) J.-T. Wang, Y. Pan, L.-M. Zhang, S.-Q. Yu, Chin. J. Chem. Phys. 20 (2007) 395–400.
[31] (a) D. Rehm, A. Weller, Ber. Bunsen-Ges. Phys. Chem. 73 (1969) 834–839;
(b) D. Rehm, A. Weller, Isr. J. Chem. 8 (1970) 259–271.
[32] (a) M. Lucarini, G.F. Pedulli, A. Alberti, C. Paradisi, S. Roffia, J. Chem. Soc., Perkin Trans. 2 (1993) 283–287;
(b) A. Streitwieser Jr., I. Schwager, J. Phys. Chem. 66 (1962) 2316–2320;
(c) S. Bonafede, M. Ciano, F. Bolletta, V. Balzani, L. Chassot, A. Von Zelewsky, J. Phys. Chem. 90 (1986) 3836–3841.
[33] (a) P.J. Wagner, R.J. Truman, A.E. Puchalski, R. Wake, J. Am. Chem. Soc. 108 (1986) 7727–7738;
(b) J.B. Guttenplan, S.B. Cohen, J. Am. Chem. Soc. 94 (1972) 4040–4042.
[34] T. Werner, J. Phys. Chem. 83 (1979) 320–325.
[35] P.B. Merkel, J.P. Dinnocenzo, J. Photochem. Photobiol. A: Chem. 193 (2008) 110–121.
[36] (a) R.E. Connors, W.R. Christian, J. Phys. Chem. 86 (1982) 1524–1528;
(b) M. Baba, T. Kamei, M. Kiritani, S. Yamauchi, N. Hirota, Chem. Phys. Lett. 185 (1991) 354–358;
(c) Y. Ohshima, T. Fujii, T. Fujita, D. Inaba, M. Baba, J. Phys. Chem. A 107 (2003) 8851–8855.
[37] K. Bartl, A. Funk, M. Gerhards, Chem. Phys.Chem. 10 (2009) 1882–1886.
[38] R. Kuhlmann, W. Schnabel, Angew. Makromol. Chem. 57 (1977) 195–210.
[39] N. Hoffmann, H. Görner, Chem. Phys. Lett. 383 (2004) 451–455.
[40] J.M. Figuera, R. Sastre, A. Costela, I. Garcia-Moreno, M.T. Al-Hakakk, J. Dabrio, Laser Chem. 15 (1994) 33–46.
[41] G. Porter, M.R. Topp, Proc. R. Soc. Lond., Ser. A 315 (1970) 163–184.
[42] See Refs. [1–38] in Supplementary material which are related to photoreduction of aromatic ketones.